crystals

MDPI

Article

Study on the Fabrication and Acoustic Properties of Near-Stoichiometric Lithium Tantalate Crystal Surface Acoustic Wave Filters

Jiashun Si [1,2,3], Xuefeng Xiao [1,2,3,*], Yan Huang [1,2,3], Yan Zhang [1,2,3], Shuaijie Liang [1,2,3], Qingyan Xu [1,2,3], Huan Zhang [1,2,3], Lingling Ma [1,2,3], Cui Yang [1,2,3] and Xuefeng Zhang [1,4]

[1] Key Laboratory of Physics and Photoelectric Information Functional Materials Sciences and Technology, North Minzu University, Wenchang Road 204, Yinchuan 750021, China
[2] College of Electric and Information Engineering, North Minzu University, Wenchang Road 204, Yinchuan 750021, China
[3] Microelectronics and Solid-State Electronics Device Research Center, North Minzu University, Yinchuan 750021, China
[4] Ningxia Ju Jing Yuan Crystal Technology, Co., Ltd., Shahu Road 304, Shizuishan 753000, China
* Correspondence: xuefengxiao@nmu.edu.cn

Abstract: Near-stoichiometric lithium tantalate (NSLT) wafers with different Li contents were prepared by vapour transfer equilibrium (VTE) method and fabricated into surface acoustic wave filters. The temperature coefficient of frequency, insertion loss, and bandwidth of the surface acoustic wave filters were tested using a special chip test bench and a network analyzer. The results show that the temperature coefficient of frequency shows a trend of first decreasing and then increasing with the increase in Li content, and the temperature stability of the surface acoustic wave filters is best when the Li content is 49.75%. It is also found that the surface acoustic wave filter fabricated from NSLT wafers has 21.18% lower temperature coefficient of frequency, 7.3% lower insertion loss, and 2.8% lower bandwidth than those fabricated from congruent lithium tantalate wafers. Therefore, NSLT crystals are more suitable for applications in acoustic devices, providing a new idea for performance enhancement of 5G communication devices.

Keywords: lithium tantalate; surface acoustic wave; filter

Citation: Si, J.; Xiao, X.; Huang, Y.; Zhang, Y.; Liang, S.; Xu, Q.; Zhang, H.; Ma, L.; Yang, C.; Zhang, X. Study on the Fabrication and Acoustic Properties of Near-Stoichiometric Lithium Tantalate Crystal Surface Acoustic Wave Filters. *Crystals* **2024**, *14*, 400. https://doi.org/10.3390/cryst14050400

Academic Editors: Luis M. Garcia-Raffi and Yutaka Fujimoto

Received: 3 April 2024
Revised: 19 April 2024
Accepted: 23 April 2024
Published: 25 April 2024

1. Introduction

Lithium tantalate ($LiTaO_3$, LT) crystals are well known for their low acoustic loss, high-voltage electrical coupling coefficient, and excellent electro-optic properties [1–4]. Therefore, this material is widely used in the fabrication of surface acoustic wave (SAW) filters. In recent years, 5G technology has gradually matured, and 5G communication devices have also been preliminarily introduced. With the improvement in 5G communication device functions, such devices face more and more clutter [5]; it has been shown that small duplexers based on LT structure have longer lives [6–8], so the miniaturization of the device and the optimization of its performance is also imminent.

Currently, the best way to reduce the size of the SAW filter is wafer-level packaging technology; of course, to realize the application, it is necessary to reduce the temperature coefficient of frequency (TCF). A large TCF can cause frequency shift when the device is too hot [5], which can seriously affect the performance of communication equipment. There are two main methods to reduce the TCF. One is to improve the technology of making SAW filters, for example, by making bulk acoustic wave filters based on multilayer film technology, which produces bulk acoustic wave filters with a very small TCF; however, the cost is very expensive [9–11]. The second is to reduce the thermal expansion

coefficient of the substrate material. The main method is to use wafer bonding technology or to find new materials that are more suitable for making SAW filters [12–16]. In wafer bonding technology, a material with negative TCF is bonded to a material with positive TCF. For example, bonding a LT wafer with a negative TCF to a Si wafer will drastically reduce the TCF of SAW filters. However, wafer bonding needs to be carried out under high vacuum and requires the use of a wafer bonding machine, which is still expensive although its cost has been reduced slightly compared to the multilayer film technology, and the bonding power is lower [17,18]. Courjon et al. [19] bonded a Y42° LT wafer to a (100) Si wafer by Au/Au bonding technology and prepared leaky surface acoustic wave (LSAW) resonators. The absolute value of the TCF can be lower than 10 ppm/K. However, the process of bonding solid non-homogeneous materials is complex and can cause irreversible damage to the wafers. In 2020, Tanaka et al. [20] made acoustic wave devices using ultrathin LT wafers (0.4 μm), which showed a significant improvement in performance, but their mechanical fragility problem led to low yield in experiments and the need for careful handling. Yet, ultrathin LT acoustic wave devices will play an important role in the 5G and post-5G era. Kadota et al. [21] confined shear horizontal waves in a thin LT structure made of a quartz substrate and fabricated hetero acoustic layer SAW resonators yielded a positive TCF with an impedance ratio of up to 84 dB and spurious-free characteristics. In 2022, Chen et al. [22] prepared wafer-level LT on quartz substrates using ion-cutting technology, and the TCF of the SAW resonator prepared by them reached −25.21 ppm/°C. Better TCF characteristics can be achieved by optimizing the cutting angle and thickness of quartz, but the lack of high-quality quartz substrates is one of the reasons limiting their large-scale fabrication of SAW filters.

The commonly used LT crystals in the market are congruent LT (CLT) crystals with Li:Ta = 48.75:51.15. The Czochralski method is the most commonly used method for growing LT crystals [23,24]. As the Li/Ta ratio in CLT crystals continues to increase and gradually approaches the stoichiometric ratio (1:1), many of their properties are improved to varying degrees. NSLT crystals are a new material with better performance. According to our research on NSLT wafers, NSLT wafers with Li content of 49.63–49.75% have fewer defects and better physical properties [25,26]. Therefore, the performance of SAW filters based on NSLT wafers may be even better. The methods for growing NSLT crystals are the double-crucible Czochralski method [27], K_2O cosolvent method [28] and VTE method [29], etc. The VTE method has the advantages of simple preparation and high-quality NSLT wafers compared with other methods. In the VTE method, the CLT wafers are placed in Li-rich LT polycrystalline materials, and under high temperature conditions, Li is transferred from the powder to the wafers by vapor transport and solid state diffusion to make NSLT wafers.

LT crystals with piezoelectric effects can achieve electroacoustic and acoustic–electric conversion. By designing the width of the interdigital transducer, the reserved wavelength can be determined, thereby achieving the filtering of clutter [30,31]. The propagation characteristics of SAW are mainly determined by the following parameters: acoustic velocity, electromechanical coupling coefficient (K^2) of the piezoelectric substrate, TCF, and quality factor [32,33]. To improve the performance of SAW filters, it is mainly necessary to increase the acoustic velocity and K^2 and reduce the TCF. Both the acoustic velocity and the TCF are related to the defect density of the SAW filter substrate material. Therefore, improving the performance of the SAW filter substrate material can effectively improve SAW filter performance. SAW filters fabricated based on Y36° CLT wafers have a lower TCF (typically −32 ppm/°C) [34], but their surface acoustic velocity is smaller and their K^2 is lower, resulting in lower acoustic–electric conversion efficiency. On the other hand, SAW filters based on Y42° CLT wafers have higher TCF (typically −42 ppm/°C) [35], but their surface sound velocity is higher and their K^2 is larger [1]. Two types of tangential wafer each have unique application advantages, so six types of SAW filters are fabricated in this paper, three of which are based on Y36° NSLT crystals with different Li contents, one of which is based on Y42° NSLT crystals, and two of which are based on CLT crystals,

in their respective tangential control groups. We studied their parameters such as TCF, insertion loss, and bandwidth, and it is demonstrated that the SAW filters based on NSLT wafers are superior to the SAW filters based on CLT wafers. The development of this work is beneficial for improving the performance of SAW filters, reducing costs, and improving the performance of SAW filters for 5G communication equipment applications.

2. Experiment

2.1. Sample Preparation

CLT crystals of Y36° and Y42° were grown by the Czochralski method. The Czochralski method was used to grow CLT crystals at a Czochralski rate of 0.3 mm/hr at 20 r/min with a melt fraction of 48.75 mol% Li_2O. Y36° NSLT wafers with different Li contents were prepared by the VTE method. Li_2CO_3 (99.99%, Jiangxi Dongpeng New Materials Co., Ltd., Jiangxi, China) and Ta_2O_5 (99.99%, Ningxia Jinbaikang Science and Technology Co., Ltd., Ningxia, China) were mixed uniformly in a certain ratio, and LT polycrystalline materials with different Li contents were made by high-temperature sintering to be used as the diffusion materials. The CLT wafer and the diffusion material were alternately put into a ceramic crucible, heated to above 1200 °C in a high-temperature furnace, and held for 50 h to complete the process of Li-ion diffusion into the wafer, and made into NSLT wafer. The Curie temperature was measured, and the Li content was determined to be 49.34%, 49.75%, and 49.91%, respectively, by the equation of Curie temperature versus Li content [25]. Y42° NSLT crystals with 49.8% Li content were also prepared. The crystal orientation and Li content of the prepared wafers are shown in Table 1.

Table 1. Crystal orientation and Li content of wafers.

Crystal Orientation	Crystal	Li Concent. (%)
Y36°	CLT	48.75
	NSLT	49.34
		49.75
		49.91
Y42°	CLT	48.75
	NSLT	49.8

2.2. Surface Acoustic Wave Filter Fabrication

The prepared NSLT wafers were thinned to 0.50 mm, and the NSLT wafers were polarized using the liquid electrode method [36] to change their multi-domain structure into a single-domain structure, which in turn enhanced the SAW speed of sound and piezoelectric constant of the NSLT wafers. The aluminum film was evaporated on the surface of the NSLT wafer using the evaporation method [37], and the thickness of the coated aluminum film was 100 nm. The photoresist was coated on the surface of the NSLT wafer, and the thickness of the photoresist was 800 nm, and it was baked at a temperature of 110 °C for 3 min to fix the photoresist. The wafers were exposed under ultraviolet light, developed in the exposed area, and the wafers were immersed in acetone to remove the excess aluminum film.

SAW filters were fabricated using NSLT crystals as the substrate material, an aluminum film was coated on the substrate, and the performance of the SAW filters was characterized. In this experiment, we made a single-port oscillator filter, and the fabrication process is shown in Figure 1, using 120 interdigital pairs and 20 electrodes on each side as the reflective end. The acoustic aperture was set to 40 λ, the interdigital and electrode distance was 1.2 μm, and the metal duty cycle was 0.5.

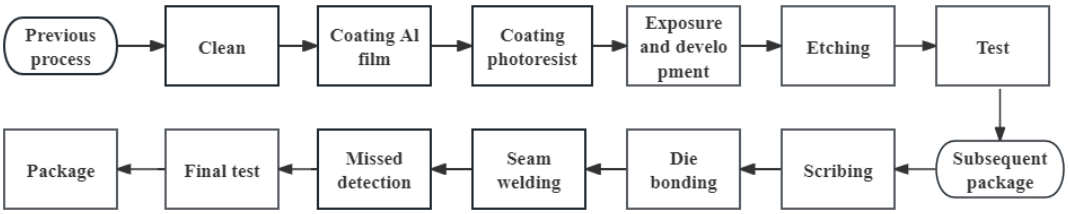

Figure 1. Steps for making SAW filters.

The fabrication of the chip was completed by the Ningxia SAW Technology Company Limited (Ningxia, China) after a series of processes such as coating, photolithography, and other processes to complete the fabrication of the SAW filter. A specific diagram is shown in Figure 2.

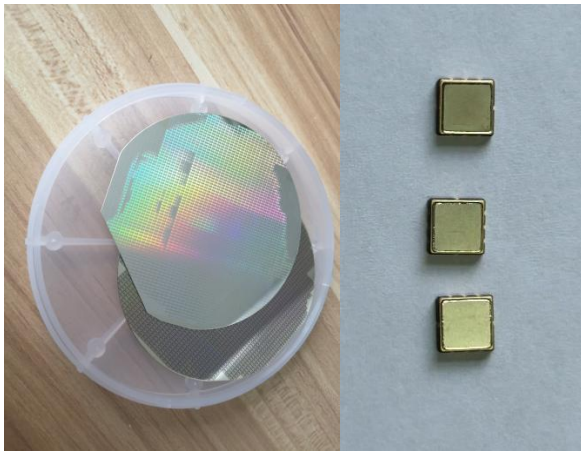

Figure 2. Photolithography (3 inches) and SAW filters (5 × 5 mm, high degree <1.5 mm).

2.3. Acoustic Performance Testing

The frequency, insertion loss, and bandwidth of the output of each SAW filter were tested at different temperatures and specific frequencies using a special chip test bench, a temperature controled box (Hangzhou Zhuochi Instrument Co. Ltd., Hangzhou, China), and a network analyzer (8712ET, Agilent, California, America). The test system is shown in Figure 3. The filter was placed on the chip test bench, and then, it was put into the temperature-controlled box, which was set in the range of 30 to 110 °C. Every 10 °C, the temperature was kept warm for half an hour, the center frequency displayed on the network analyzer was recorded, and the TCF was calculated from the frequency.

(**a**) (**b**)

Figure 3. Acoustic Performance Test System (**a**) network analyzer, (**b**) temperature controled box.

3. Results and Discussion

3.1. Temperature Coefficient of Frequency

Temperature changes will cause hermal expansion of the NSLT substrate of the SAW filter. The thermal expansion of the wafer leads to changes in the surface acoustic velocity of the substrate, which in turn affects the center frequency of the SAW filter and the efficiency in filtering out spurious waves [26]. For many precision communication devices, such as mobile phones and electronic computers, the excellent performance of these devices can only be ensured by completely filtering out the SAW in other frequency bands and retaining the waves in the desired frequency bands. With the development of communication equipment, the number of SAW filters in communication equipment is increasing, resulting in smaller and smaller spacing between different filtering frequency bands. Therefore, a smaller TCF helps to improve the performance of communication equipment.

In this paper, the TCF of the packaged SAW filter is tested. The calculation formula for TCF is shown in (1) [38]:

$$TCF \approx \frac{1}{f_0}\frac{df}{dT}, \quad (1)$$

where f_0 is the center frequency at room temperature.

Table 2 shows the TCF of SAW filters based on Y36° NSLT wafers with different Li contents as substrates. According to Table 2, the TCF of SAW filters based on CLT crystals is −34.85 ppm/°C, which is higher than that of SAW filters based on NSLT crystals. The relationship between Li content and TCF is shown in Figure 4. It can be seen from Figure 4 that the TCF of the fabricated SAW filter shows a tendency of decreasing and then increasing as the Li content of the wafers increases and reaches the optimum at a Li content of 49.75%.

Table 2. TCF of SAW filters.

Li Content in Y36° Wafers (%)	CLT (48.75)	NSLT (49.34)	NSLT (49.75)	NSLT (49.91)
TCF of SAW filters (ppm/°C)	−34.85	−32.93	−25.68	−27.5

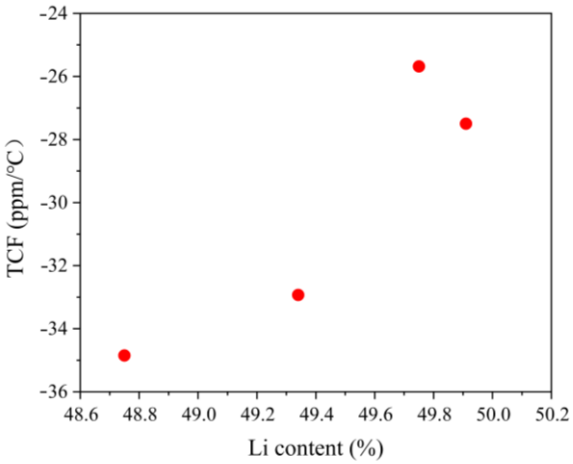

Figure 4. Scatter plot of the relationship between Li content and TCF.

In this paper, SAW filters based on Y42° CLT and NSLT wafers were also fabricated. Table 3 shows the TCF of SAW filters based on Y42° CLT and NSLT wafers. The center frequency of the input acoustic wave is 220 MHz. The output frequency of the other end of the SAW filter was tested using a network analyzer, and the test results are shown in

Table 3 and Figure 5. The equations for the fitted curves in Figure 5 are (a) y = 216.97663 − 0.00912x and (b) y = 218.96308 − 0.00819x, respectively. The TCF of two SAW filters was calculated based on the above equation. The TCF of the SAW filter based on the Y42° CLT wafer was −41.45 ppm/°C, which is very close to the theoretical value of −42 ppm/°C. The TCF of the SAW filter based on the Y42° NSLT wafer was −37.23 ppm/°C, which is 10.18% lower than that based on Y42° CLT wafer. The TCF of the SAW filter has been greatly reduced.

Table 3. TCF.

Temperature (°C)		SAW Filter (CLT)	SAW Filter (NSLT)
Center frequency (MHz)	30	216.697	218.709
	40	216.604	218.638
	50	216.513	218.563
	60	216.42	218.476
	70	216.338	218.389
	80	216.247	218.310
	90	216.155	218.223
	100	216.073	218.140
	110	215.975	218.061
Theoretical value (ppm/°C)		−42	
Measured value (ppm/°C)		−41.45	−37.23

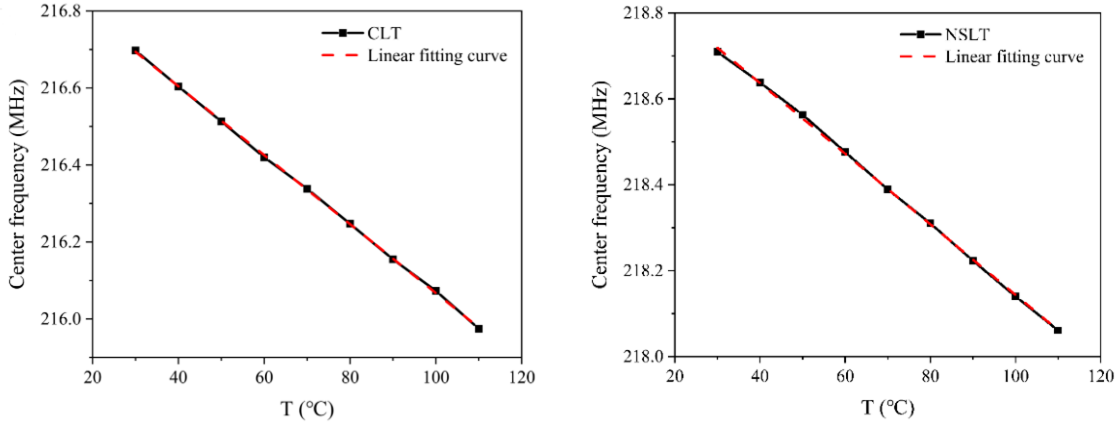

(**a**) (**b**)

Figure 5. Linear fitting curve between center frequency and temperature of SAW filter (**a**) CLT wafer, (**b**) NSLT wafer.

3.2. Insertion Loss

Insertion loss refers to the change in output power caused by the use of SAW filters in transmission systems, i.e., the output signal has a small attenuation relative to the input signal. The calculation formula is shown in (2) [39]:

$$IL = -10\log(P_0/P_i), \quad (2)$$

where IL is the insertion loss, P_0 is the output power, and P_i is the input power. According to the formula, the larger the insertion loss, the lower the energy transfer efficiency. For SAW filters, the smaller the insertion loss, the better the device performance.

Table 4 shows the insertion loss of SAW filters based on CLT and NSLT wafers. It can be seen from Table 4 that as the temperature increases, the insertion loss of the SAW filters based on the two wafers will increase. At 30 °C, the insertion loss of the SAW filters based on CLT and NSLT wafers is 2.24 dB and 2.27 dB, respectively; at 110 °C, the insertion loss

of the SAW filters based on CLT and NSLT wafers is 3.02 dB and 2.64 dB, respectively. At room temperature, the insertion loss of the two SAW filters is similar, but as the temperature increases, the insertion loss of the SAW filter based on CLT wafers increases more.

In summary, the insertion loss of the SAW filter based on NSLT wafers is lower than that of the SAW filter based on CLT wafers, and its input and output energy conversion ratios are higher.

Table 4. Insertion loss.

	Temperature (°C)	SAW Filter (CLT)	SAW Filter (NSLT)
Insertion loss (dB)	30	2.24	2.27
	40	2.35	2.3
	50	2.39	2.32
	60	2.48	2.31
	70	2.55	2.37
	80	2.70	2.42
	90	2.78	2.47
	100	2.83	2.55
	110	3.02	2.64
	average value	2.59	2.40

3.3. Bandwidth

Bandwidth refers to the width of the frequency band through which a signal can pass, i.e., the difference between the highest frequency and the lowest frequency of the current band [14]. High-generation communication devices such as those using 5G will have more and more communication bands, and in addition to upgrading the communication bands, another means is to reduce the bandwidth.

The bandwidth of the SAW filters was tested using a network analyzer, and its bandwidth values are shown in Table 5. According to Table 5, the average bandwidth of the SAW filter based on Y42° CLT crystal is 7.859 MHz, while the average bandwidth of the SAW filter based on Y42° NSLT crystal is 7.635 MHz. That is to say, the average bandwidth of the SAW filter based on Y42° NSLT crystal is 2.8% smaller than that of the SAW filter based on Y42° CLT crystal.

Table 5. Bandwidth.

	Temperature (°C)	Y42° CLT	Y42° NSLT (49.80%)
SAW filters bandwidth (MHz)	30	7.873	7.633
	40	7.863	7.600
	50	7.851	7.607
	60	7.855	7.599
	70	7.860	7.633
	80	7.858	7.639
	90	7.863	7.643
	100	7.861	7.666
	110	7.849	7.699
	average value	7.859	7.635

4. Summary

In this paper, SAW filters were fabricated based on CLT and NSLT wafers. The TCF, insertion loss and bandwidth of the SAW filters were tested, and the relationship between Li content and TCF was analyzed. Through testing the TCF of Y36° NSLT wafers with different Li contents, it was concluded that the TCF first decreases and then increases with

the increase in Li content, and the TCF of the SAW filter reaches the optimum when the Li content inside the NSLT crystal is 49.75%. The TCF, average insertion loss, and average bandwidth of the SAW filters fabricated based on the Y42° CLT wafer and the Y42° NSLT wafer were also tested. Compared with the SAW filter based on CLT wafers, the TCF of the SAW filter based on NSLT wafers was decreased by 21.18%, the insertion loss was decreased by 7.3%, and the bandwidth was decreased by 2.8%. In summary, the performance of SAW filters based on NSLT wafers is superior to those based on CLT wafers.

Author Contributions: Conceptualization, X.X., Q.X. and X.Z.; methodology, X.Z.; validation, X.X.; formal analysis, J.S. and Q.X.; investigation, X.X., Y.H., Y.Z., S.L., H.Z., L.M. and C.Y.; data curation, J.S., S.L. and Q.X.; writing—original draft preparation, J.S.; writing—review and editing, J.S. and X.X.; funding acquisition, X.X., H.Z. and X.Z. All authors have read and agreed to the published version of the manuscript.

Funding: This work is supported by the Ningxia key Natural Science Foundation project (2023AAC02045), the National Natural Science Foundation of China (61965001, 11864001, and 61461001), the Fundamental Research Funds for the Central Universities, North Minzu University (2021KJCX07), the Ningxia Province Key Research and Development Program (2018BEE03015, 2021BEE03005, and 2022BFE02009), the Natural Science Foundation of Ningxia (2019AAC03103, 2020AAC03239, and 2023AAC03304), and the Ningxia first-class discipline and scientific research projects (electronic science and technology, No. NXYLXK2017A07-DKPD2023C10 and DKPD2023D01).

Data Availability Statement: The raw data supporting the conclusions of this article will be made available by the authors on request.

Acknowledgments: The authors thank the Key Laboratory of North Minzu University (Physics and Photoelectric Information Functional Materials Sciences and Technology), the Ningxia Advanced Intelligent Perception Control Innovation Team, the Ningxia Acousto-optic Crystals Industrialization Innovation Team, and the Ningxia New Solid Electronic Materials and Devices Research and Development Innovation Team (2020CXTDLX12), as well as Hong Zhang, Zhijuan Zhao, and Shunjing Lei of Ningxia SAW Technology Co., Ltd. for their assistance in acoustic testing.

Conflicts of Interest: Author Xuefeng Zhang is employed by Ningxia Ju Jing Yuan Crystal Technology, Co., Ltd. The remaining authors declare that the research was conducted in the absence of any commercial or financial relationships that could be construed as a potential conflict of interest.

References

1. Kawachi, O.; Mineyoshi, S.; Endoh, G.; Ueda, M.; Ikata, O.; Hashimoto, E.; Yamaguchi, M. Optimal cut for leaky SAW on $LiTaO_3$ for high performance resonators and filters. *IEEE Trans. Ultrason. Ferroelectr. Freq. Control* **2001**, *48*, 1442–1448. https://doi.org/10.1109/58.949755.
2. Smith, R.; Welsh, F. Temperature dependence of the elastic, piezoelectric, and dielectric constants of lithium tantalate and lithium niobate. *J. Appl. Phys.* **1971**, *42*, 2219–2230. https://doi.org/10.1063/1.1660528.
3. Kuznetsova, I.E.; Zaitsev, B.D.; Joshi, S.G.; Borodina, I.A. Investigation of acoustic waves in thin plates of lithium niobate and lithium tantalate. *IEEE Trans. Ultrason. Ferroelectr. Freq. Control* **2001**, *48*, 322–328. https://doi.org/10.1109/58.896145.
4. Shibata, Y.; Kuze, N.; Matsui, M.; Kanno, Y.; Kaya, K.; Ozaki, M.; Kanai, M.; Kawai, T. Surface acoustic wave properties of lithium tantalate films grown by pulsed laser deposition. *Jpn. J. Appl. Phys.* **1995**, *34*, 249. https://doi.org/10.1143/JJAP.34.249.
5. Warder, P.; Layus, N. Selecting filters for challenging mobile applications worldwide. *Microw. J.* **2013**, *56*, 96.
6. Yang, J.; Mao, Q.; Shang, J.; Hao, H.; Li, Q.; Huang, C.; Zhang, L.; Sun, J. Preparation and characterization of thick stoichiometric lithium tantalate crystals by vapor transport equilibration method. *Mater. Lett.* **2018**, *232*, 150–152. https://doi.org/10.1016/j.matlet.2018.08.105.
7. Tsutsumi, J.; Inoue, S.; Iwamoto, Y.; Miura, M.; Matsuda, T.; Satoh, Y.; Nishizawa, T.; Ueda, M.; Ikata, O. A miniaturized 3/spl times/3-mm SAW antenna duplexer for the US-PCS band with temperature-compensated $LiTaO_3$/sapphire substrate. In Proceedings of the IEEE Ultrasonics Symposium, Montreal, QC, Canada, 23–27 August 2004. https://doi.org/10.1109/ULTSYM.2004.1417917.
8. Murata, T.; Kadota, M.; Nakao, T.; Matsuda, K.; Hashimoto, K.-Y. Improvement of shape factor and loss of surface acoustic wave resonator filter composed of SiO_2/high-density-electrode/$LiTaO_3$. *Jpn. J. Appl. Phys.* **2009**, *48*, 07GG05. https://doi.org/10.1143/JJAP.48.07GG05.
9. Lakin, K.M. Thin film resonators and filters. In Proceedings of the 1999 IEEE Ultrasonics Symposium Proceedings International Symposium (Cat No 99CH37027), San Diego, CA, USA, 27–29 October 1982. https://doi.org/10.1109/ULTSYM.1999.849135.

10. Lakin, K.M.; Kline, G.R.; Mccarron, K.T. Development of miniature filters for wireless applications. *IEEE Trans. Microw. Theory Tech.* **1995**, *43*, 2933–2939. https://doi.org/10.1109/22.475658.
11. Kline, G.; Lakin, K.; Mccarron, K. Overmoded high Q resonators for microwave oscillators. In Proceedings of the 1993 IEEE International Frequency Control Symposium, Salt Lake City, UT, USA, 2–4 June 1993. https://doi.org/10.1109/FREQ.1993.367467.
12. Hashimotoky, K.M. Recent development of temperature compensated SAW devices. *Proc. IEEE Ultrason. Symp.* **2011**, *79*, 86. https://doi.org/10.1109/ULTSYM.2011.0021.
13. Kao, K.; Cheng, C.; Chen, Y.; Chen, C. The dispersion properties of surface acoustic wave devices on AlN/$LiNbO_3$ film/substrate structure. *Appl. Surf. Sci.* **2004**, *230*, 334–339. https://doi.org/10.1016/j.apsusc.2004.02.049.
14. Onishi, K.; Namba, A.; Sato, H.; Ogura, T.; Seki, S.; Taguchi, Y.; Tomita, Y.; Kawasaki, O.; Eda, K. A novel temperature compensation method for SAW devices using direct bonding techniques. In Proceedings of the 1997 IEEE Ultrasonics Symposium Proceedings An International Symposium, Toronto, ON, Canada, 5–8 October 1997. https://doi.org/10.1109/ULTSYM.1997.663015.
15. Sato, H.; Onishi, K.; Shimamura, T.; Tomita, Y. Temperature stable SAW devices using directly bonded $LiTaO_3$/glass substrates. In Proceedings of the 1998 IEEE Ultrasonics Symposium Proceedings, Sendai, Japan, 5–8 October 1998. https://doi.org/10.1109/ULTSYM.1998.762159.
16. Miura, M.; Matsuda, T.; Ueda, M.; Satoh, Y.; Ikata, O.; Ebata, Y.; Takagi, H. Temperature compensated $LiTaO_3$/sapphire SAW substrate for high power applications. In Proceedings of the IEEE Ultrasonics Symposium, Rotterdam, The Netherlands, 18–21 September 2005. https://doi.org/10.1109/ULTSYM.2005.1602917.
17. Parker, T.; Schulz, M.; Wichansky, H. Temperature stable materials for SAW devices. In Proceedings of the 29th Annual Symposium on Frequency Control, Atlantic City, NJ, USA, 28–30 May 1975. https://doi.org/10.1109/FREQ.1975.200076.
18. Nakai, Y.; Nakao, T.; Nishiyama, K.; Kadota, M. Surface acoustic wave duplexer composed of SiO_2 film with convex and concave on Cu-electrodes/$LiNbO_3$ structure. In Proceedings of the 2008 IEEE Ultrasonics Symposium, Beijing, China, 2–5 November 2008. https://doi.org/10.1109/ULTSYM.2008.0385.
19. Courjon, E.; Ballandras, S.; Daniau, W.; Baron, T.; Moulet, J.; Signamarcheix, T. $LiTaO_3$/silicon composite wafers for the fabrication of low loss low TCF high coupling resonators for filter applications. In Proceedings of the 2015 Joint IEEEISAF, ISIF, and PFM, Singapore, 24–27 May 2015. https://doi.org/10.1109/ISAF.2015.7172709.
20. Tanaka, S.; Kadota, M. IDT-based acoustic wave devices using ultrathin lithium niobate and lithium tantalate. In Proceedings of the 2020 Joint Conference of the IFCS-ISAF, Keystone, CO, USA, 19–23 July 2020; pp. 1–3. https://doi.org/10.1109/IFCS-ISAF41089.2020.9234811.
21. Kadota, M.; Ishii, Y.; Tanaka, S. Surface acoustic wave resonators with hetero acoustic layer (HAL) structure using lithium tantalate and quartz. *IEEE Trans. Ultrason. Ferroelectr. Freq. Control* **2020**, *68*, 1955–1964. https://doi.org/10.1109/TUFFC.2020.3039471.
22. Chen, Y.; Wu, J.; Zhao, X.; Li, Z.; Ke, X.; Zhang, S.; Zhou, M.; Huang, K.; Ou, X. Heterogeneous integration of lithium tantalate thin film on quartz for high performance surface acoustic wave resonator. *Jpn. J. Appl. Phys.* **2022**, *62*, 015503. https://doi.org/10.35848/1347-4065/aca5d7.
23. Ballman, A.A. Growth of piezoelectric and ferroelectric materials by the CzochraIski technique. *J. Am. Ceram.* **1965**, *48*, 112–113. https://doi.org/10.1111/j.1151-2916.1965.tb11814.x.
24. Ohno, Y.; Kubouchi, Y.; Yoshida, H.; Kochiya, T.; Kajigaya, T. Twinning in Czochralski-Grown 36°-RY $LiTaO_3$ Single Crystals. *Crystals* **2020**, *10*, 1009. https://doi.org/10.3390/cryst10111009.
25. Xiao, X.; Xu, Q.; Liang, S.; Zhang, H.; Ma, L.; Hai, L.; Zhang, X. Preparation and defect structure analysis of near-stoichiometric lithium tantalate wafers. *RSC Adv.* **2022**, *12*, 19091–19100. https://doi.org/10.1039/D2RA02775E.
26. Xiao, X.; Xu, Q.; Liang, S.; Zhang, H.; Ma, L.; Hai, L.; Zhang, X. Preparation, electrical, thermal and mechanical properties of near-stoichiometric lithium tantalate wafers. *J. Mater. Sci.-Mater. Electron.* **2022**, *33*, 20668–20677. https://doi.org/10.1007/s10854-022-08878-3.
27. Kitamura, K.; Yamamoto, J.K.; Iyi, N.; Kirnura, S.; Hayashi, T. Stoichiometric LiNbO3 single crystal growth by double crucible Czochralski method using automatic powder supply system. *J. Cryst. Growth* **1992**, *116*, 327–332. https://doi.org/10.1016/0022-0248(92)90640-5.
28. Jia, B.; Zhao, Y. Near stoichiometric lithium tantalate crystal growth and its periodic polarization. *Acta Opt. Sin.* **2010**, *30*, 3249–3252.
29. Bordui, P.F.; Norwood, R.G.; Bird, C.D.; Carella, J.T. Stoichiometry issues in single-crystal lithium tantalate. *J. Appl. Phys.* **1995**, *78*, 4647–4650. https://doi.org/10.1063/1.359811.
30. Campbell, C. *Surface Acoustic Wave Devices for Mobile and Wireless Communications, Four-Volume Set*; Academic Press: Cambridge, MA, USA, 1998.
31. Morgan, D. *Surface Acoustic Wave Filters: With Applications to Electronic Communications and Signal Processing*; Academic Press: Cambridge, MA, USA, 2010. https://doi.org/10.1016/B978-0-12-372537-0.X5000-6.
32. Campbell, C. *Surface Acoustic Wave Devices and Their Signal Processing Applications*; Elsevier: Amsterdam, The Netherlands, 2012. https://doi.org/10.1016/B978-0-12-157345-4.X5001-2.
33. Dvoesherstov, M.Y.; Petrov, S.; Cherednik, V.; Chirimanov, A. The temperature coefficients of delay of surface acoustic waves in LGS and LGN crystals in a wide temperature range. *Tech. Phys.* **2001**, *46*, 346–347. https://doi.org/10.1134/1.1356488.

34. Yamanouch, K. High coupling and zero TCF SH-SAW and SH-Boundary SAW using electrodes/Rotated YX $LiTaO_3$ and SiO_2/electrodes/Rotated YX $LiTaO_3$. In Proceedings of the 2013 IEEE IUS, Prague, Czech Republic, 21–25 July 2013. https://doi.org/10.1109/ULTSYM.2013.0272.
35. Kadota, M.; Nakao, T.; Taniguchi, N.; Takata, E.; Mimura, M.; Nishiyama, K.; Hada, T.; Komura, T. SAW substrate, with coupling factor and excellent temperature stability suitable for duplexer of PCS in US. In Proceedings of the IEEE Ultrasonics Symposium, Montreal, QC, Canada, 23–27 August 2004. https://doi.org/10.1109/ULTSYM.2004.1418219.
36. Busacca, A.; Cherchi, M.; Sanseverino, S.R.; Cino, A.C.; Parisi, A.; Assanto, G.; Cichoki, M.; Caccavale, F.D.; Morbiato, A. Surface periodic poling in lithium niobate and lithium tantalate. In Proceedings of the 2005 IEEE/LEOS Workshop on Fibres and Optical Passive Components, Palermo, Italy, 22–24 June 2005. https://doi.org/10.1109/WFOPC.2005.1462112.
37. Smith, H.I.; Bachner, F.J.; Efremow, N. A High-Yield Photolithographic Technique for Surface Wave Devices. *J. Electrochem. Soc.* **1971**, *118*, 821. https://doi.org/10.1149/1.2408173.
38. Zhang, G.; Wenkang, S.; Xiaojun, J.; Tao, H.; Feng, D.; Lianger, L. Temperature characteristics of surface acoustic waves propagating on $La_3Ga_5SiO_4$ substrates. *J. Mater. Sci. Technol.* **2004**, *20*, 63.
39. Ballandras, S.; Steichen, W. Composants acoustiques utilisés pour le filtrage-Modèles et outils de simulation. **2010**. https://doi.org/10.51257/a-v1-e2001.